ELSEVIER

Solid State Ionics 140 (2001) 293–300

SOLID STATE IONICS

www.elsevier.com/locate/ssi

Silver intercalation in $PbS_{1.18}(TiS_2)_n$, $n = 1, 2$, misfit layer compounds

Alexander N. Titov [a], Ingrid Bryntse [b], Svetlana G. Titova [c,*], Nadezhda V. Toporova [a]

[a] Urals State University, 620083 Ekaterinburg, Russia

[b] Department of Inorganic Chemistry, Arrhenius Laboratory, Stockholm University, S-106-91 Stockholm, Sweden

[c] Institute of Metallurgy, Urals Division of Russian Academy of Sciences, Amundsen St. 101, Ekaterinburg 620016, Russia

Received 7 June 2000; received in revised form 27 November 2000; accepted 23 February 2001

Abstract

The reaction between metallic Ag and $PbS_{1.18}(TiS_2)_n$, $n = 1$, 2, misfit layer compounds has been investigated by electrochemical technique, X-ray powder analysis and transmission electron microscopy. It was found that silver intercalation is possible only in the compound with $n = 2$. The thermodynamic behavior and location of phase boundaries were studied in the temperature range 400–650 K. DC-conductivity and magnetic-susceptibility measurements were performed, and the data can be interpreted as an appearance of small polarons during silver insertion. © 2001 Elsevier Science B.V. All rights reserved.

MAT: Ag; $PbS_{1.18}(TiS_2)$; $PbS_{1.18}(TiS_2)_2$

PACS: 71.20.T; 71.38

Keywords: Intercalation; Misfit layer compounds; Polarons

1. Introduction

Misfit layer compounds are built up of one or two sheets of transition metal dichalcogenide, TX_2, alternating with one double layer of another MX (M = Pb, Sn, Bi, Sb, rare earth metal) monochalcogenide. In general, such compounds may be considered as resulting from insertion of an MX layer into a TX_2 network (X = S, Se). This insertion leads to distortion of the main lattice so that an incommensurate modulation of the crystal structure forms along the *a*-axis [1]. The general formula is often written $(MX)_m(TX_2)_n$, where m is an irrational number and n is 1 or 2.

The misfit compounds may be intercalated by several alkali metals, which make them interesting for applications such as electrode materials in electrochemical devices. For instance, Hernan et al. [2] performed Li intercalation of $(PbS)_{1.18}(TiS_2)_n$, $n = 1$, 2, and used this phase to create a battery with a weak dependence of EMF on the degree of discharge.

The limit of metal atoms, which may be inserted to reach an equilibria with the host material, is influenced by the conduction band capacity for the TX_2 part, which is determined mainly by its degree of filling by electrons transferred from the MX part. These factors also influence the chemical bond character between the TX_2 and MX parts. For M = Pb,

* Corresponding author. Tel.: +7-3432-678909; fax: +7-3432-286130.

E-mail address: titova@imet.sco.ru (S.G. Titova).

PII: S0167-2738(01)00825-6

Sn the MX-layer was reported to have a not noticeable ionization degree and the bond character was unclear. Moelo et al. [3] concluded that the attraction between these layers stem from a formation of charged defects in the MX-layer due to a substitution of Ti^{3+} for Pb^{2+}, accompanied by an electron transfer in the conduction band of TX_2. This conclusion was based on composition analysis, which showed a systematic overestimation of the transition metal concentration compared to the expected metal ratio. On the other hand, an occupation of Ti^{3+} at the TX_2/MX interlayer would lead to the same result. Therefore, in order to establish the origin of the chemical bond, it is necessary to know whether or not this boundary is available for insertion. For example, Hernan et al. [2] reported that Li was successfully intercalated into the TX_2/MX interlayer in $(PbS)_{1.18}(TiS_2)_n$, in contrast to Lavela et al. [4] who claim that it is not possible to insert Na at this boundary in $(PbS)_{0.59}TiS_2$.

In this work, we have investigated electrochemical silver intercalation into $(PbS)_{1.18}(TiS_2)$, which does not possess a Van der Waals gap, and into $(PbS)_{0.59}(TiS_2)$, which contains one VdW gap per unit cell. The properties of the synthesized materials were investigated in order to establish whether or not these interlayer spacings could function as hosts for inserted Ag.

2. Experimental

The materials $(PbS)_{0.59}TiS_2$ (the same as $(PbS)_{1.18}(TiS_2)_2$) and $(PbS)_{1.18}TiS_2$ were prepared by reacting initially prepared TiS_2, S (99.995%, high purity) and Pb (purity 99.95%) in sealed silica ampoules. After annealing at 900°C for 2 weeks, the charges were crushed, pressed and annealed again under the same conditions to ensure homogeneity. The materials obtained were checked by X-ray powder analysis, using a DRON-4-13 diffractometer (Cu k_α-radiation, graphite monochromator).

An electrochemical technique, using AgI as solid electrolyte in the cell $Ag|AgI|Ag_x(PbS)_{0.59}TiS_2|Pt$, was used for intercalation of silver into $(PbS)_{0.59}TiS_2$, $(PbS)_{1.18}TiS_2$ as well as into the individual materials TiS_2 and PbS. The location of phase boundaries in the x–T plane (x is the silver content in $Ag_x(PbS)_{0.59}TiS_2$ and $Ag_x(PbS)_{1.18}TiS_2$) was determined measuring the EMF (E) of the electrochemical cell as a function of the silver content and the temperature, as described previously [5].

The atom content of the $(PbS)_{0.59}TiS_2$ samples before and after Ag intercalation was analysed by energy-dispersive spectrometry (EDS) in a JEOL 2000FX transmission electron microscope (TEM), using the *L*-lines for Ag and Pb and the *K*-lines for Ti and S. Selected-area electron diffraction (ED) patterns of the analysed crystallites were also obtained. Immediately before the TEM investigations, the sample to be studied was crushed in a mortar. The crystallites were then placed on a metal grid covered with a support film of amorphous carbon. Two routes were tried: either mortaring inside a dry box without adding any solvent or quickly crushing the particles in an organic solvent, such as xylene, in ambient atmosphere.

The magnetic susceptibility of the silver-intercalated misfit compounds was measured with a Faraday balance in the temperature range 77–300 K. The DC conductivity was measured by the four-probe technique in the temperature range 80–650 K.

3. Results and discussion

The synthesized pristine materials were quite homogeneous. The X-ray powder pattern of $(PbS)_{1.18}TiS_2$ was indexed according to the space group $C2/m$, which gave the same unit cell constants as reported by Wiegers et al. [1]. The X-ray powder pattern of $(PbS)_{0.59}TiS_2$ was the same as reported earlier by Meerschaut et al. [6], and the unit cell was also confirmed by a tunneling electron microscopy (TEM) study. Typical selected-area electron diffraction patterns of pristine $(PbS)_{0.59}TiS_2$ were found to resemble ED patterns of similar misfit compounds reported by Hernan et al. [2] and by Kuypers et al. [7]. Measurements of the a^*-axis, as outlined in Fig. 1, of the PbS unit cell gave $a \approx 5.57$ Å. Assuming an orthorhombic cell for the pseudohexagonal TiS_2 unit cell, the corresponding a^*-axis was measured and gave $a \approx 3.34$ Å. The ratio $m = a_{TiS_2}/a_{PbS}$ was calculated to 0.60, which corroborates the formula

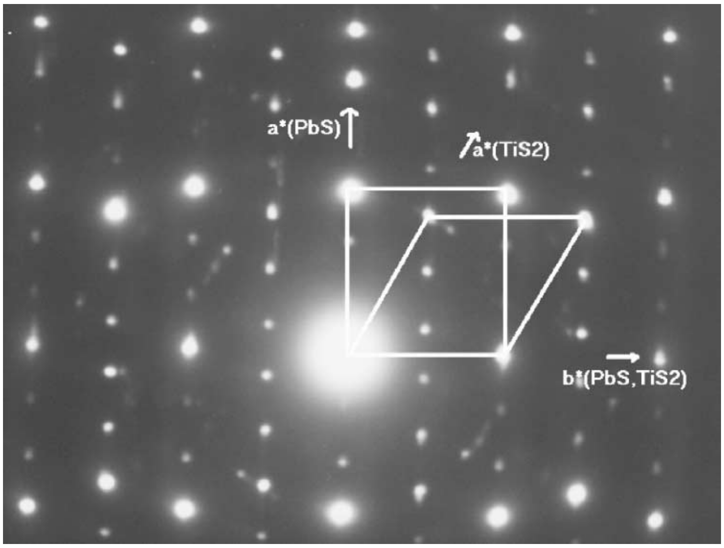

Fig. 1. Selected-area electron diffraction pattern of the $a^* b^*$ projection of pristine $(PbS)_{0.59}TiS_2$. The reciprocal lattice of the nearly cubic PbS and the pseudo-hexagonal TiS_2 structure parts are outlined in the figure.

$(PbS)_{0.59}TiS_2$ with $m = 0.59$ (see the structure projections in Ref. [7]). EDS analysis of thin fragments yielded an element ratio of Pb:Ti:S = 12.4(5):22(1):65(1), with standard deviations within parentheses. Assuming the number of S atoms to be fixed at 2.59, the formula according to EDS would be $Pb_{0.5(2)}Ti_{0.88(4)}S_{2.59}$, which also agrees fairly well with the gross composition.

The reaction $x\mathrm{Ag} + (\mathrm{PbS})_{1.18}\mathrm{TiS}_2$ was found to be irreversible. For $x < 0.03$, the dependence $E(x)$ is the same as for the reaction $x\mathrm{Ag} + \mathrm{PbS}$, which is described below. For larger x-values, $x > 0.03$, $E(x) =$ constant, equal to the EMF of $Ag_x(PbS)_{0.59}TiS_2$ for $0 < x < 0.25$. This allows us to conclude that intercalation of silver into $(PbS)_{1.18}TiS_2$ leads to a decomposition of the misfit compound:

$$x\mathrm{Ag} + (\mathrm{PbS})_{1.18}\mathrm{TiS}_2 = \mathrm{Ag}_x(\mathrm{PbS})_{0.59}\mathrm{TiS}_2 + 0.59\mathrm{PbS}.$$

This interpretation is supported by X-ray powder diffraction analysis of $(PbS)_{1.18}TiS_2$ after silver insertion, which showed that this sample contains significant amounts of PbS and $(PbS)_{0.59}TiS_2$ (Fig. 2).

The concentration dependence of the EMF (E) of the electrochemical cell, measured at 473 K, for $Ag_x(PbS)_{0.59}TiS_2$ and TiS_2, respectively, is shown in Fig. 3. The silver solubility in PbS is approximately 10^5 times less than in a TiS_2-containing material (10^{-4} mol% at a sulphur pressure of 0–10^5 Pa and $T = 773$ K [8]). Moreover, the diffusion coefficient of silver in PbS is very low in the considered temperature range (10^{-10} cm^2/s at 773 K [8]), and the accuracy of the obtained data is rather poor;

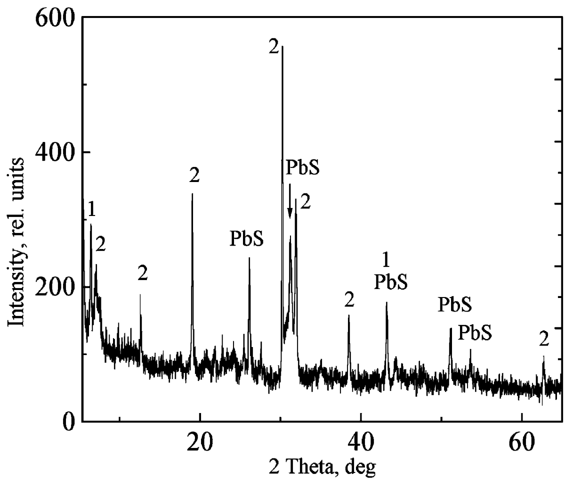

Fig. 2. The X-ray powder diffraction pattern of $(PbS)_{1.18}TiS_2$ (1) after silver insertion. Except of the main phase, reflections of PbS and $Ag_x(PbS)_{0.59}TiS_2$ (2) are shown.

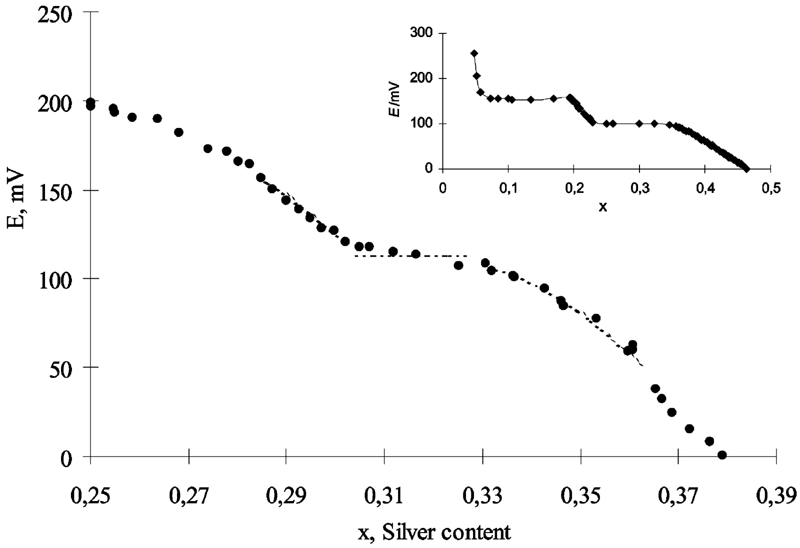

Fig. 3. The dependence of EMF on silver content x for $Ag_x(PbS)_{0.59}TiS_2$. EMF vs. x for Ag_xTiS_2 is shown in the insert.

therefore we have not included these data in the figure. At the same time, the EMF of the electrochemical Ag\AgI\PbS cell at 200°C has the stable, well-defined value 280 mV. Interestingly, the EMF of the Ag\AgI\$(PbS)_{1.18}TiS_2$ cell is the same. To explain this fact, we suggest that silver atoms are inserted into all decomposition products of $(PbS)_{1.18}TiS_2$:PbS, TiS_2 and $(PbS)_{0.59}TiS_2$. The measured EMF value corresponds to the reaction Ag + PbS with higher potential.

The electrochemical titration curve for silver intercalation in $Ag_x(PbS)_{0.59}TiS_2$ is reversible during injection/extraction cycles. This allows us to conclude that the reaction between silver and $(PbS)_{0.59}TiS_2$ is an intercalation process:

$$x\mathrm{Ag} + (\mathrm{PbS})_{0.59}\mathrm{TiS}_2 = \mathrm{Ag}_x(\mathrm{PbS})_{0.59}\mathrm{TiS}_2.$$

The decomposition of $(PbS)_{1.18}TiS_2$, in contrast to the stability of $Ag_x(PbS)_{0.59}TiS_2$ during the reaction with silver, suggests that the Ag atoms are mainly situated between neighboring TiS_2 layers in the same way as in other intercalated TiX_2 compounds.

At a silver content of $x \approx 0.38$, an equilibrium between $Ag_x(PbS)_{0.59}TiS_2$ and bulk silver was obtained. Two single-phase areas were found: $0.33 < x < 0.38$ (I) and $0.25 < x < 0.30$ (II). For both these areas, no initial compounds were detected by X-ray phase analysis. The values of the unit-cell constants for all investigated materials are summarized in Table 1. The a-axes for the TiS_2-part, for compounds with

Table 1
Unit cell parameters of metal sulfides in the system $Ag_x(PbS)_nTiS_2$ obtained by X-ray powder diffraction

	a (Å)	b (Å)	c (Å)	β
TiS_2 (JSPDS 15-0853)	3.407		5.695	
PbS (JSPDS 5-0592)	5.9362			
$Ag_{0.25}TiS_2$ [17]	3.416		12.145	
$Ag_{0.4}TiS_2$ [17]	3.437		6.445	
$(PbS)_{1.18}TiS_2$ [a]				
PbS-part	5.800	5.881	11.76	95.28
TiS_2-part	3.409	5.881	11.76	95.28
$(PbS)_{0.59}TiS_2$ [a]				
PbS-part	5.761	5.873	17.464	93.62
TiS_2-part	3.390	5.873	17.464	93.62
$Ag_{0.25}(PbS)_{0.59}$-TiS_2 [b]	13.717(5)	5.835(4)	17.484(5)	94.33(3)
PbS-part	5.611(3)	5.865(2)	17.49(6)	94.13(6)
$Ag_{0.25}TiS_2$-part	3.387(1)	5.861(4)	17.35(6)	93.85(6)
$Ag_{0.38}(PbS)_{0.59}$-TiS_2 [b]	13.929(5)	5.824(6)	17.565(5)	94.35(3)
PbS-part	5.631(4)	5.879(3)	17.51(3)	93.9(2)
$Ag_{0.4}TiS_2$-part	3.443(1)	5.845(2)	17.409(4)	94.3(2)

[a] The parameters of these samples were reported in Ref. [1].
[b] The parameters calculated without refinement of atom coordinates.

and without silver, were calculated by assuming that the cell parameters of the PbS part remained constant after the Ag intercalation. It may be noted that the obtained a parameters of the TiS_2 part in $Ag_x(PbS)_{0.59}TiS_2$ are very close to the cell parameters for Ag_xTiS_2 with the same silver content, see Table 1.

In Table 1, the unit cell parameters for PbS- and TiS_2-parts of $Ag_x(PbS)_{0.59}TiS_2$ are shown. At a small increase of silver, x, the a-axis of PbS-part slightly decreases while the a-axis of the TiS_2-part remains constant. Probably, the interaction of these structural fragments with silver occurs by the same way as in case of a mechanical mixture of bulk PbS and TiS_2 materials: due to the favorable formation energy of $Ag_xPb_{1-x}S$, the PbS-part solves all silver at a small silver concentration ($x < 0.25$). When the PbS-part is saturated, the silver atoms start to intercalate into the TiS_2-part. Therefore, for a silver content $x > 0.25$ the a-axis for PbS remains nearly constant while the a-axis for the TiS_2-part starts to increase.

EDS analysis in the TEM was performed on two of the Ag-intercalated $Ag_x(PbS)_{0.59}TiS_2$ samples. The sample with a high initial silver content, $Ag_{0.38}(PbS)_{0.59}TiS_2$, achieved a calculated formula of $Ag_{0.3(1)}Pb_{0.44(2)}Ti_{0.89(4)}S_{2.59}$. Besides the major phase, small amounts of '$Ag_{0.06}TiS_2$' were identified during the microscope investigation. EDS analysis of the sample with gross composition $Ag_{0.25}(PbS)_{0.59}TiS_2$ gave a fairly similar formula of $Ag_{0.26(4)}Pb_{0.45(3)}Ti_{0.87(3)}S_{2.59}$. In this sample, another more Ag-rich phase was found with the approximate formula '$Ag_{0.4}TiS_2$'. Thus, by this TEM/EDS investigation, it was not possible to find any significant difference between the Ag intercalated samples with initial compositions $Ag_{0.38}(PbS)_{0.59}TiS_2$ and $Ag_{0.25}(PbS)_{0.59}TiS_2$.

The most typical selected-area electron diffraction pattern of the a^*b^* projection of $Ag_{0.25}(PbS)_{0.59}TiS_2$ is shown in Fig. 4. The image is similar to the ED pattern in Fig. 1 belonging to $(PbS)_{0.59}TiS_2$. In both ED patterns, the strong reflections stem either from the PbS or from TiS_2 individual parts, as indicated in Fig. 4. Besides, weak reflections appear that are caused by the whole misfit structure. For example, the reflection marked with * in the latter figure can be regarded as the difference between the vectors 200(PbS) and $100(TiS_2)$. The ratio between the lattice parameters, a_{TiS_2}/a_{PbS}, calculated manually or by the program ELD [9], was similar, within the accuracy of the method, to the one of the pristine phase $(PbS)_{0.59}TiS_2$. In contradiction to the results of Hernan et al. [2], we very seldom observed a change of orientation of the PbS part relative to the TiS_2

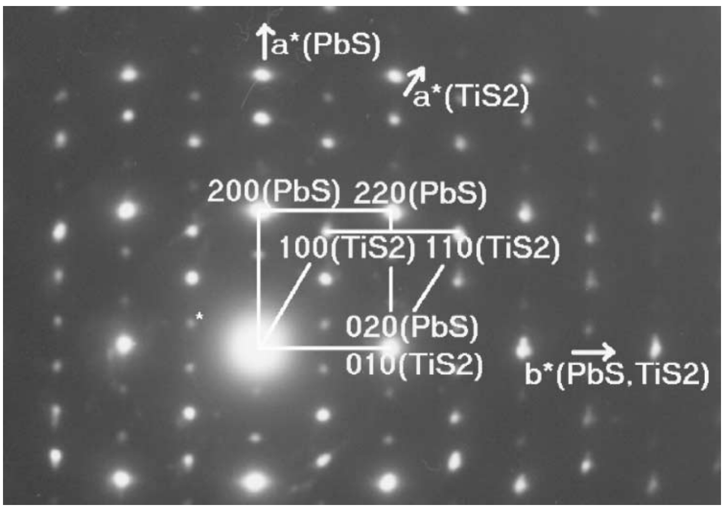

Fig. 4. Selected-area electron diffraction pattern for $Ag_x(PbS)_{0.59}TiS_2$, $x = 0.4$. The reciprocal lattice of the nearly cubic PbS structure part and the pseudo-hexagonal TiS_2 structure part are outlined. The PbS indices are marked above the reflections and the TiS_2 indices are marked below the corresponding reflections. The weak reflections, such as the one indicated *, belong to the whole misfit layer structure.

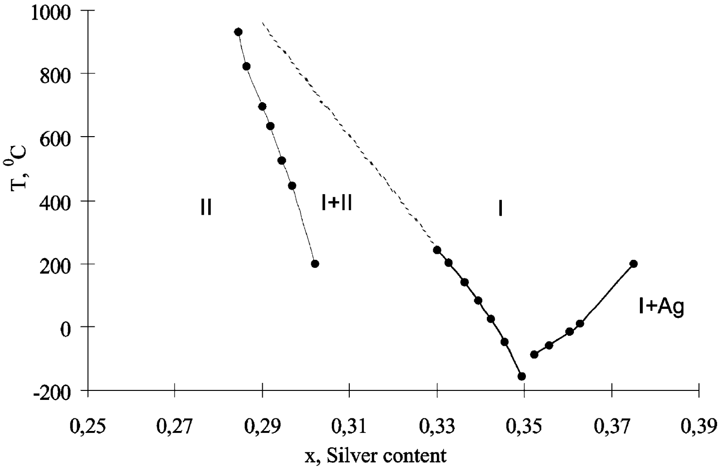

Fig. 5. Phase diagram of $Ag_x(PbS)_{0.59}TiS_2$, $x = 0.35$—triple point: equilibrium of I and II phase and Ag. At $x = 0.25$, the temperature dependence of the phase boundary has not been investigated. The location of boundaries of single-phase regions was obtained as a set of points of an intersection of temperature dependence of EMF of electrochemical cell for two-phase and single phase regions. Single-phase boundaries obtained by this way are shown by solid line. We also have extrapolated the 'directly' obtained boundary 'Phase 1'/Mixture ('Phase 1' + 'Phase 2') to the high-temperature region (dashed line).

part. This might be connected with a different type of interlayer distribution of intercalated Ag and Li in the misfit $(PbS)_{0.59}TiS_2$ material. Quite a few disordered or nearly amorphous ED patterns were found. However, the appearance was more or less the same whether or not the crystals were crushed in an organic solvent before being placed on a grid for electron microscopy.

In summary, by this TEM study, it is not possible to detect any structural difference between pristine and Ag intercalated $(PbS)_{0.59}TiS_2$ or to locate exactly where the silver atoms are placed. However, the EDS analysis supports that the examined crystallites from the intercalated phase do contain Ag.

The temperature dependence of EMF of the electrochemical cell for different silver contents was obtained in the interval 420–650 K. From these data, the phase boundaries were established for areas I and II in the (T, x) plane, see Fig. 5. The obtained phase diagram is very similar to the low-temperature part of the diagram for Ag_xTiS_2 [5]. The absence of a single-phase region with silver content $x \approx 0$ may be a consequence of strong interaction between inserted silver atoms and the host lattice, as observed for Ag_xTiTe_2 and Ag_xTiSe_2 [5,10]. The maximum content of intercalated silver in $Ag_x(PbS)_{0.59}TiS_2$ is close to that in Ag_xTiS_2. This fact is in accordance with the conclusion about negligible charge transfer between the PbS and TiS_2 parts.

The magnetic susceptibility as a function of temperature for pristine $(PbS)_{0.59}TiS_2$, as well as the intercalated compounds with $x = 0.35$, 0.40 (phase I) and 0.25 (phase II) is shown in Fig. 6. The pristine material shows a Pauli-like behavior of the suscepti-

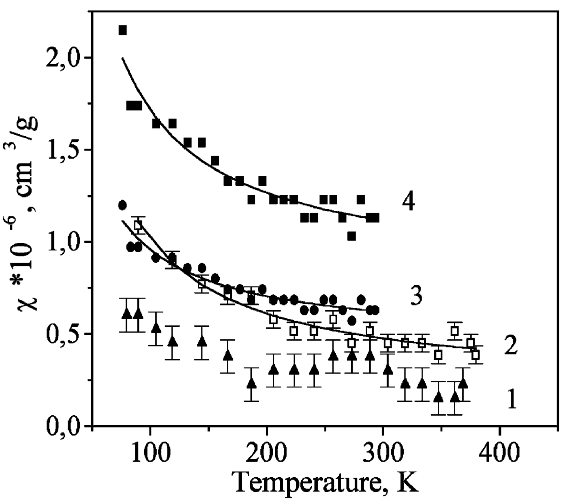

Fig. 6. Temperature dependence of the magnetic susceptibility for $Ag_x(PbS)_{0.59}TiS_2$: (1) $x = 0$, (2) $x = 0.25$, (3) $x = 0.35$, and (4) $x = 0.38$.

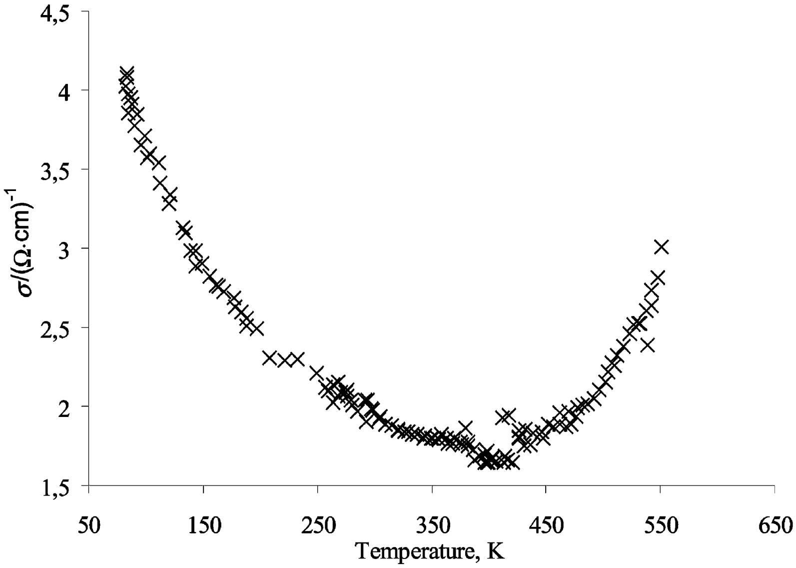

Fig. 7. Electrical conductivity vs. temperature for $Ag_{0.27}(PbS)_{0.59}TiS_2$.

bility, with $\chi(T) = \text{const}$, within the accuracy of the method. The weak Curie–Weiss term for this composition may be connected with a small amount of Ti in the Van der Waals gap, as observed for TiS_2 [11]. The intercalated materials demonstrate a $\chi \sim C/(T - \theta)$ dependence. The best fit was obtained for this law with $\theta = 0$. As only Ti atoms may have a magnetic moment, this behavior is probably connected with the appearance of Ti^{3+} ions. However, the concentration of Ti^{3+} ions calculated from the $\chi(T)$ dependence is about two to three times less than the concentration of intercalated silver. As an interpretation of concentration and temperature dependence of magnetic susceptibility, we therefore suggest the existence of a narrow band of Ti *3d* states at the Fermi level, as previously reported for Ag_xTiTe_2 [10] and Ag_xTiSe_2 [12].

The temperature dependence of the electrical conductivity for $Ag_x(PbS)_{0.59}TiS_2$ was measured for materials with silver content $0 < x < 0.38$. Both temperature dependences and values of conductivity were similar for all measured samples. A typical curve for $Ag_{0.27}(PbS)_{0.59}TiS_2$ (phase II) is shown in Fig. 7. The change of conductivity type from metallic to temperature activated occurs at $T \approx 400$ K. In general, such behavior with minimum of conductivity is typical when small polarons act as charge carriers [13]. We suggest that the narrow band of Ti *3d* states, as noted above, has a polaronic origin. If we suppose that these polarons are connected with Ti–Ag–Ti bonds, as described for many M_xTiX_2 (M = Ag, Co, Fe; X = Se, Te) compounds [14–16], the difficulty of such bond formation in $(PbS)_{1.18}TiS_2$ may be a reason why intercalates of this phase cannot be obtained. The situation is different for Li-intercalated $Li_x(PbS)(TiS_2)_n$, ($n = 1, 2$) [3], since a Li insertion was neither reported to lead to a noticeable lattice distortion nor to an appearance of polarons.

Acknowledgements

This work was supported by the Russian Foundation for Basic Research, Grant no. 98-03-32656a and the Swedish Natural Science Research Council (NFR).

References

[1] G.A. Wiegers, A. Meerschaut, in: A. Meerschaut (Ed.), Material Science Forum 100 & 101, “Incommensurate Sandwiched Layered Compounds”, Trans. Tech. Publ., Uetikon-Zuerich, 1992, p. 101.

[2] L. Hernan, P. Lavela, J. Morales, J. Pattanayak, J.L. Tirado, Mater. Res. Bull. 26 (1991) 1211.
[3] Y. Moelo, A. Meerschaut, J. Rouxel, C. Auriel, Chem. Mater. 7 (1995) 1759.
[4] P. Lavela, J. Morales, J.L. Tirado, J. Solid State Chem. 124 (1996) 238.
[5] A.N. Titov, S.G. Titova, Phys. Solid State 37 (2) (1995) 310.
[6] A. Meerschaut, C. Auriel, J. Rouxel, J. Alloys Compd. 183 (1992) 129.
[7] S. Kuypers, J. VanLanduyt, S. Amelinckx, J. Solid State Chem. 86 (1990) 212.
[8] M.V. Slinkina, Investigation of silver diffusion machanism in lead and cadmium sulfides, PhD Thesis, Ural State Univ., Sverdlovsk, 1982.
[9] S. Hovmöller, Ultramicroscopy 41 (1992) 121.
[10] A.N. Titov, Inorg. Mater. 33 (1997) 447.
[11] J.A. Wilson, Phys. Status Solidi B 86 (1978) 11.
[12] V.M. Antropov, A.N. Titov, L.S. Krasavin, Phys. Solid State 38 (1996) 713.
[13] A.S. Alexandrov, N.F. Mott, Polarons and Bipolarons, World Scientific Publishing, Singapore, 1995.
[14] V.G. Pleshchev, A.N. Titov, S.G. Titova, A.V. Kuranov, Phys. Solid State 39 (1997) 1442.
[15] V.G. Pleshchev, A.N. Titov, S.G. Titova, A.V. Kuranov, Inorg. Mater. 33 (1997) 1128.
[16] A.N. Titov, A.V. Dolgoshein, Phys. Solid State 40 (1998) 1081.
[17] G.A. Sholz, R.F. Frindt, Mater. Res. Bull. 15 (1980) 1703.